INFLUENCE OF RESIDUAL STRESSES, GENERATED DURING PRECRACKING, IN STRESS CORROSION TESTS

A.M. Lancha and M. Elices*

Slow strain rate tests on precracked samples have shown that test severity depends on fatigue loads during precracking, although fatigue loads were well below maximum values recommended by Standards. Test severity, measured as percentage of rupture load in solution with respect to rupture load in air, increases as fatigue load decreases. Extension and shape of TTS fracture area appears to be related with compressive residual stresses induced during fatigue precracking.

INTRODUCTION

A well developed philosophy has arisen relating to the use of fatigue precracked specimens for stress corrosion testing; the use of precracked specimens, for instance, can show those environments where stress corrosion cracking (SCC) will **not** occur on smooth specimens, since if SCC does not occur in the presence of severe stress concentrators it will surely not occur in their absence. Another aspect, worth considering, is the simulation of local pH and potential inside crack that is otherwise difficult to reproduce with smooth or notched specimens.

This technique has been applied succesfully to test SCC of wires under constant load, McGuinn and Elices (1) and under constant slow strain rate, Parkins et al. (2). However, test results showed certain unavoidable scatter.

This paper presents some preliminary results of work being done to ascertain the source of scatter. It seems that residual stresses, induced during fatigue precracking, may well be the origin of differences in test results otherwise obtained in the same conditions.

* Materials Science Department. E.T.S. Caminos. Universidad Politécnica de Madrid. 28040-MADRID. SPAIN

EXPERIMENTAL PROCEDURE

The material used was a commercial 12 mm diameter eutectoid pearlitic steel rod. This steel was patented by cooling from the austenitic condition in a molten lead bath to produce fine pearlite. Chemical composition and mechanical properties are shown in Table 1.

TABLE 1 - Composition and Mechanical Properties.

C %	Mn %	Si %	P %	S %	UTS MPa	%PS MPa	El* %
0.74	0.70	0.20	0.016	0.023	1176	725	8

* Elongation at maximum load.

The specimens were transverse precracked rods, in which a starter notch, some 1 mm in depth, was introduced with a jewellers file (figure 1). The transverse pre-crack was produced by axial fatigue. To ensure sharp cracks which were readily reproducible the stress intensity factor range was adjusted so that the last 1 mm of crack propagation involved not less than 40000 cycles. Samples were coated with an insulating lacquer except for a band about 1 mm wide on each side of the notch and pre-crack.

The specimens were subjected to slow strain rate testing, Parkins (3). The crosshead speed was 8.3×10^{-8} ms^{-1}, based on previous experience (2). The specimens were subjected to fractographic assessment after failure, but quantification of the extent of the effects of the environmental conditions on fracture was conveniently achieved through the ratio of the maximum load achieved in the test environment to that in a test in air.

The test environment was an aqueous solution of 1 gl^{-1} $Ca(OH)_2$ plus 0.1 gl^{-1} NaCl to which HCl was added in varying amounts to adjust the pH value below the value of 12.5 for the base solution. Testing was performed at ambient temperature (between 16 and 22 C).

All tests were performed at constant potential set by means of an electronic potentiostat and a classical three electrode assembly, as described elsewhere (2).

To ascertain severity of fatigue precracking, different types of samples were prepared. Fracture toughness, K_C, was measured using a method developed for cyclindrical specimens, Astiz et al. (4). Such procedure yields valid K_{IC} plane strain fracture toughness, for this steel up to temperatures of about 0 C, Elices (5), and it is suspected that the measured temperature value, $K_C = 53$ MPa $m^{1/2}$, is not far from

K_{IC}. A first series was precracked with loads not exceeding 0.60 K_C, as recommended by most standards. Two more sets of samples were prepared precracking at loads not exceeding 0.45 K_C and 0.28 K_C, well below requirements. Finally another series at higher loads, 0.80 K_C, was done for comparison purposes.

EXPERIMENTAL RESULTS

The results from tests employing transverse pre-cracked specimens in solutions of initial pH 12.5, 8 and 4 are shown in figures 2, 3 and 4 respectively. It appears that marked sensitivities to environment fracture becomes noticeable at potentials below about -900 mV (SCE) for pH 12.5, -800 mV(SCE) for pH 8, and -600 mV (SCE) for pH 4. These values correspond roughly with the equilibrium values of the reaction,

$$H_2 = 2H^+ + 2e^-$$

and sensitivity to SCC below these potentials seems related to the ingress of hydrogen into the steel. A further regime of enhanced crackings appears at higher potentials.

The effect of fatigue load during precracking is similar for pH 12.5, pH 8 and pH 4; SCC is enhanced as precracking loads are lower. When precracked under higher loads, SCC may be hampered for certain potentials above hydrogen discharge values, as shown in figures 2, 3 and 4.

For potentials below hydrogen discharge, fractographic analysis always showed a small region, by the crack tip, where fracture surface has microcracks and may be classified as TTS (tearing topography surface) Thompson and Chesnut (6), Lancha (7), figure 5.The width of the TTS zone depends on potential -wider for lower potentials- and on precracking fatigue loads -high loads produce narrow TTS zones-.

DISCUSSION AND CONCLUSIONS

Slow strain rate tests on precracked samples have shown, conclusively, that test severity depends on fatigue loads during precracking. It was suspected that precracking according to ASTM E399 standard -i.e., $K_{max} \leq 0.60\ K_{IC}$- will yield samples with similar behaviour when tested in aggressive environment. Figures 2, 3 and 4 show that precracking with procedures where the maximum stress intensity factor is well below 0.6 K_{IC}, as 0.45 K_{IC} or 0.28 K_{IC}, produce samples that behave quite differently in slow strain rate tests.

Test severity, measured as percentage of rupture load in solution with respect to rupture load in air, increases as fatigue load decreases, as shown in figures 6 and 7, for two potentials. At -1200 mV (SCE), below hydrogen discharge,

test severity depends on K_{max} during fatigue precracking and is independent of pH values (figure 6). At -400 mV (SCE), well above hydrogen discharge, test severity depends on K_{max} **and** pH values; at this potential, test severity is enhanced as pH values are more acid (figure 7).

Size of TTS region is also dependent on K_{max} during fatigue precracking, as shown in figure 8 for pH = 12.5 and V = -1200 mV (SCE). The maximum width, measured at crack center, was 200 μm for the lowest available fatigue load (K_{max} = 0.28 K_C).

The presence of compressive residual stresses induced during fatigue precracking may help in understanding these results. In another paper in this conference, Toribio and Elices (8), it is shown that TTS surfaces are associated with hydrogen embrittlement in eutectoid steels when tested using this technique. It is well known that hydrogen embrittlement is enhanced by tensile stresses and hence compressive stresses will hamper growth of TTS region, as shown in figure 8 and in consequence diminish test severity. Moreover a rough estimation of plastic zone size from,

$$r_y = \frac{1}{\pi}\left(\frac{K}{Y\sigma}\right)^2$$

where Y is taken from [5], shows good agreement with measured TTS widths. Extension and shape of TTS region, jointly with knowledge of residual stress field may help in understanding, as well as modelling, hydrogen embrittlement in these steels. Work is in progress in this direction.

Another conclusion, addressed to researchers using the slow strain rate for testing precracked samples, is to warn them against residual stresses induced during fatigue precracking. Although this effect is well known for short cracks it also has to be considered when sample ligament length is very short, as happens with transverse precracked wires.

SYMBOLS USED

K	=	Stress intensity factor (Pa $m^{1/2}$)
K_C	=	Fracture toughness (Pa $m^{1/2}$)
K_{IC}	=	Plane strain fracture toughness (Pa $m^{1/2}$)
r_y	=	Plastic zone size
Y	=	Nondimensional factor in stress intensity expressions
σ	=	Stress (Pa)
SCC	=	Stress Corrosion Cracking
TTS	=	Tearing Topography Surface
SCE	=	Standard Calomel Electrode

REFERENCES

(1) McGuinn, K.F. and Elices, M., "Stress Corrosion Resistance of Transverse Precracked Prestressing Tendon in Tension", Br. Corros. J., Vol. 16, No. 4, 1981, pp. 187-195.

(2) Parkins, R.N., Elices, M., Sánchez-Gálvez, V. and Caballero, L., "Environment Sensitive Cracking of Prestressing Steels", Corrosion Science, Vol. 22, No. 5, 1982, pp. 379-405.

(3) Parkins, R.N., "Development of Strain-Rate Testing and its Implications", ASTM STP 665, 1979, pp. 5-25.

(4) Astiz, M.A., Elices, M. and Valiente, A., "Numerical and Experimental Analysis of Cracked Cylindrical Bars", in ECF 6, Proceedings, Vol. I, 1986, pp.

(5) Elices, M., "Fracture of Steels for Reinforcing and Prestressing Concrete", in Fracture Mechanics of Concrete (G.C. Sih and A. DiTommaso, Eds.), Martinus Nijhoff, 1984.

(6) Thompson, A.W. and Chesnutt, J.C., "Identification of a Fracture Mode: The Tearing Topography Surface", Met. Trans., Vol. 10A, 1979, pp. 1193-1196.

(7) Lancha, A.M., "Influencia del Trefilado en la Corrosión bajo Tensión de Aceros Eutectoides", Ph.D. Facultad de C. Químicas, Universidad Complutense de Madrid, 1987.

(8) Toribio, J. and Elices, M. "Slow Strain-Rate Technique Applied to Round-Notched Wires", in these Proceedings.

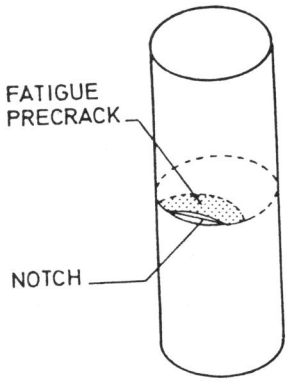

Figure 1 Specimen: Transverse precracked rod.

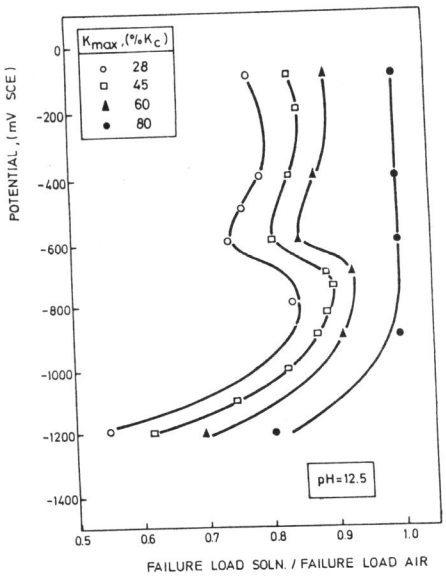

Figure 2 Constant strain rate tests: pH = 12.5.

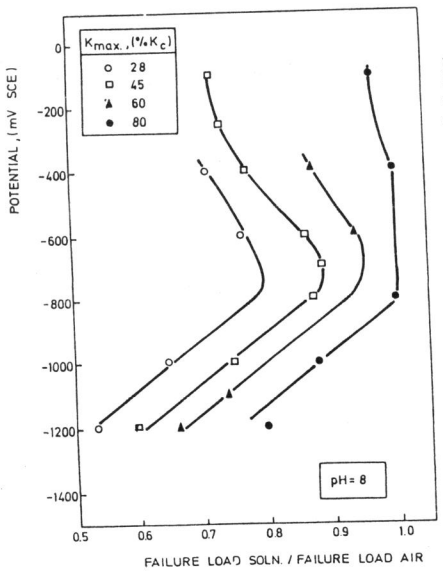

Figure 3 Constant strain rate tests: pH = 8.

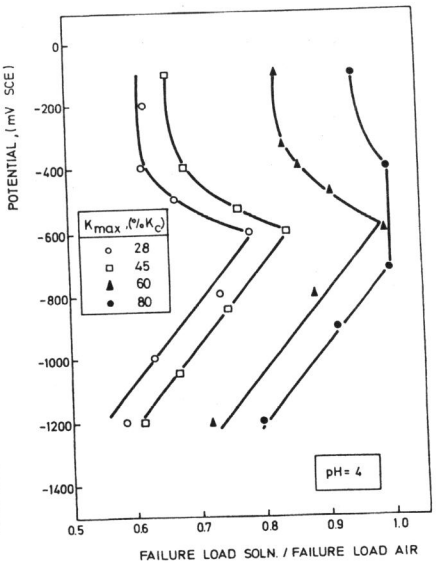

Figure 4 Constant strain rate tests: pH = 4.

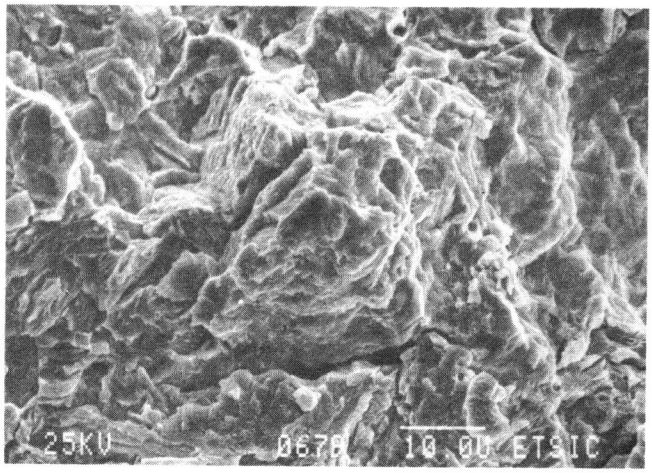

Figure 5 Tearing topography surface (TTS).

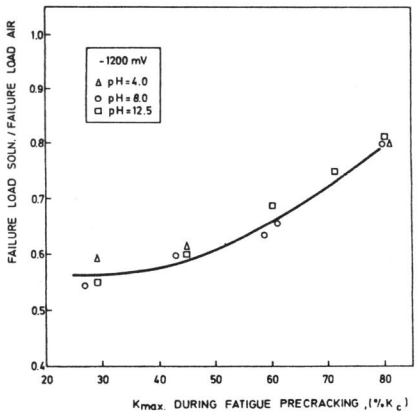

Figure 6 Test severity at -1200 mV (SCE).

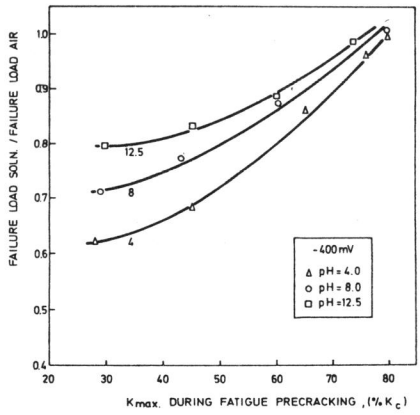

Figure 7 Test severity at -400 mV (SCE).

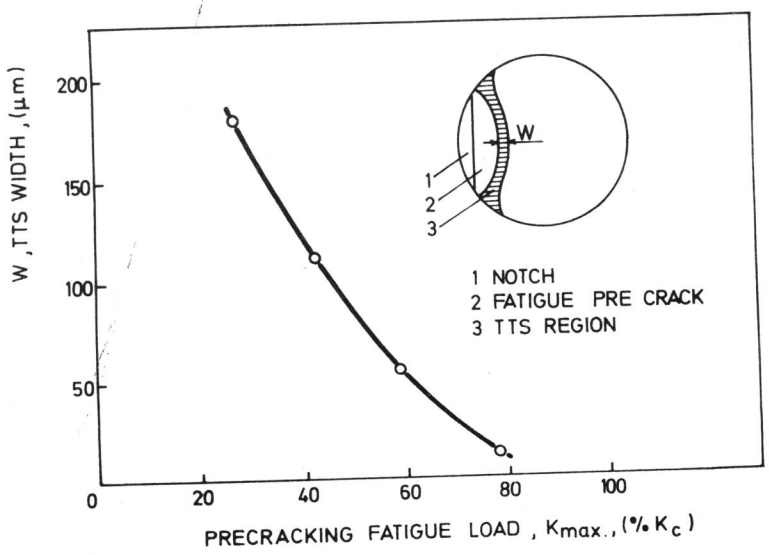

Figure 8 TTS width versus precraking fatigue load.